HOKKAIDO UNIVERSITY

Title	Jun Activation Domain-binding Protein 1 (JAB1) Is Required for the Optimal Response to Interferons
Author(s)	Muromoto, Ryuta; Nakajima, Maiko; Hirashima, Koki; Hirao, Toru; Kon, Shigeyuki; Shimoda, Kazuya; Oritani, Kenji; Matsuda, Tadashi
Citation	Journal of biological chemistry, 288(43), 30969-30979 https://doi.org/10.1074/jbc.M113.485847
Issue Date	2013-10-25
Doc URL	http://hdl.handle.net/2115/54867
Rights	This research was originally published in the Journal of biological chemistry. Muromoto R, et al. Jun activation domain-binding protein 1 (JAB1) is required for the optimal response to interferons. The Journal of biological chemistry. 2013; 288(43):30969-79. ©2013 the American Society for Biochemistry and Molecular Biology.
Type	article (author version)
File Information	WoS_64413_Matsuda_Tadashi.pdf

Instructions for use

Jun activation domain-binding protein 1 (JAB1) is required for the optimal response to interferons

Ryuta Muromoto[1], Maiko Nakajima[1], Koki Hirashima[1], Toru Hirao[1], Shigeyuki Kon[1], Kazuya Shimoda[2], Kenji Oritani[3], and Tadashi Matsuda[1]

[1]Department of Immunology, Graduate School of Pharmaceutical Sciences, Hokkaido University, Kita-12 Nishi-6, Kita-Ku, Sapporo, 060-0812, Japan
[2]Department of Gastroenterology and Hematology, Faculty of Medicine, Miyazaki University, 5200 Kihara, Kiyotake, Miyazaki 889-1692, Japan
[3]Department of Hematology and Oncology, Graduate School of Medicine, Osaka University, 2-2 Yamada-oka, Suita, Osaka 565-0871, Japan

*Running title: *JAB1 positively regulates IFN response*

To whom all correspondence should be addressed: Dr. T. Matsuda, Department of Immunology, Graduate School of Pharmaceutical Sciences, Hokkaido University, Kita-12 Nishi-6, Kita-Ku, Sapporo, 060-0812, Japan.   E-mail: tmatsuda@pharm.hokudai.ac.jp   Phone: +81-11-706-3243   Fax: +81-11-706-4990

Background: The IFN receptor (IFNR) protein level determines cellular responsiveness to IFNs.
Results: Knockdown of Jun activation domain-binding protein 1 (JAB1) resulted in the reduction of IFNR level and IFN-induced gene expression.
Conclusion: JAB1 stabilizes IFNR and is required for the optimal response to IFNs.
Significance: This study provides evidence that JAB1 positively regulates IFN response.

ABSTRACT

   Degradation of IFNR protein is one of the mechanisms to limit the extent of cellular responses to interferons. Tyrosine kinase 2 (TYK2), a JAK family kinase, has been reported to bind to and stabilize IFNR, indicating that TYK2 is a fundamental component of IFN receptor complex. Herein, we identified Jun activation domain-binding protein 1 (JAB1) as a new TYK2 binding partner and investigated its role in the regulation of IFN responses. siRNA knockdown of JAB1 resulted in suppression of IFN-induced phosphorylation of STAT proteins and their transcriptional activation. Importantly, JAB1 knockdown induced the activation of SCF ubiquitin ligase complex containing Cullin 1 (CUL1), as judged by the enhancement of covalent modification of CUL1 with the ubiquitin-like protein NEDD8, and markedly reduced the basal protein level of IFNR. In contrast, NEDD8 knockdown or inhibition of NEDD8-modification by NEDD8-activating enzyme (NAE) inhibitor resulted in increased IFNR protein concomitantly with reduction of NEDD8-modified CUL1. Furthermore, NAE inhibitor treatment enhanced the susceptibility to IFN-α in HeLa cells. These data suggest that the NEDD8 modification pathway is involved in the proteolysis of IFNAR1 and that JAB1 acts as a positive regulator of IFN responses by stabilizing IFNR through antagonizing the NEDD8 pathway.

Interferon-α (IFN-α) mediates potent antiviral and antiproliferative activities of target cells through its interaction with IFN-α receptors. Janus kinase 1 (JAK1) and Tyrosine kinase 2 (TYK2), the nonreceptor tyrosine kinases of the JAK family, are associated with IFN-α receptors and play a pivotal role in transducing IFN-α signals (1). The type I IFN receptor consists of two subunits, IFNAR1 and IFNAR2 (2). IFNAR1 plays a key role in all aspects of IFN-α-mediated effects *in vitro* and *in vivo* (3-5). Downregulation and degradation of IFNAR1 is one of the pivotal mechanisms to limit the extent and duration of cellular responses to IFN-α. Both basal- and ligand-induced turnover of IFNAR1 require its phosphorylation on Ser535 within the conserved [534]DSGNYS destruction motif (6,7). Subsequently, IFNAR1 was ubiquitinated by the SCF (Skp1, Cullin, F-box)-type E3 ubiquitin ligase complex, leading to its lysosomal degradation (6).

SCF E3 ubiquitin ligase complex is one of the most intensively studied Cullin-RING E3 ubiquitin ligases (CRLs) (8-10). Its enzyme activity is regulated by the reversible covalent modification of the Cullin subunit by the ubiquitin-like protein neural precursor cell expressed, developmentally down-regulated 8 (NEDD8) (11,12). The NEDD8 modification (neddylation) of Cullin family proteins is essential for the SCF ubiquitin ligase activity. Indeed, neddylation of CUL1 triggers ubiquitination of a substrate IκB by SCF ubiquitin ligase (13-15).

COP9 signalosome (CSN) is a protein complex consisting of eight subunits that acts in the regulation of many fundamental processes controlled by CRLs and the ubiquitin proteasome system (16-20). The best-characterized biochemical activity of CSN is the removal of NEDD8 from Cullins (deneddylation), which is catalyzed by the metalloprotease activity of the fifth subunit, CSN5 (also known as COPS5 or Jun activation domain-binding protein 1; JAB1)

(21-23).

TYK2 contributes to the IFN-induced signaling through its kinase activity leading to the phosphorylation of STAT proteins (1). Phosphorylated STATs are subsequently translocated to the nucleus, where they affect gene expression. TYK2 also stabilizes basal IFNAR1 protein expression and ligand binding ability by kinase-independent mechanisms, especially in human cells (24,25). Therefore, TYK2 is important for the IFN response as the fundamental component of the IFN receptor complex. Based on the finding that a type 2 hyper-IgE syndrome (HIES) patient was susceptible to intracellular bacterial infection and had a defect in the signal transduction of IFN-α and IL-12, human TYK2 deficiency has been identified as a molecular cause of type 2 HIES (26).

In this study, we identified that the CSN component JAB1/CSN5 is a new TYK2 binding partner. We show that JAB1 positively regulates the basal protein stability of IFNR and the IFNs response by antagonizing the neddylation pathway. This study shows the significance of JAB1 function in the optimal IFN responses in human cells.

EXPERIMENTAL PROCEDURES

Yeast two-hybrid screening–To generate a bait construct with human TYK2, PCR was used to amplify the cDNA fragment encoding amino acid residues 868-1187 (primer sequences are available upon request). The PCR product was digested with NdeI and EcoRI and inserted into pGBKT7. The bait plasmid, pGBKT7/TYK2, was stably expressed in yeast strain AH109. Y187 cells pretransformed with the human placenta Matchmaker cDNA library (Clontech Laboratories, Palo Alto, CA, USA) were used for mating. All yeast two-hybrid screening was performed as described previously (27).

Mammalian expression vector constructs–Myc-tagged TYK2 deletion mutants

2

were described previously (28). JAB1 encoding amino acids 30–334, whose gene product associated with TYK2 (aa 868–1187) in yeast, was subcloned into pCS2-MT vector. The full-length human JAB1 cDNA was purchased from Promega (Madison, WI, USA). The full-length JAB1, JAB1 D151N and JAB1 N mutants were generated by PCR and subcloned into the BamHI/EcoRI sites of the FLAG-tagged mammalian expression plasmid pSF1 (29).

Cell culture and reagents–A human cervix carcinoma cell line (HeLa), a human embryonic kidney carcinoma cell line (293T), a human hepatoma cell line (Hep3B) and human keratinocyte (HaCaT) were maintained in DMEM containing 10% Fetal Calf Serum (FCS). A human T cell leukemia cell line (Jurkat) and a human pre-B cell leukemia (NALM-6) were maintained in RPMI 1640 containing 10% FCS. Human aortic vascular smooth muscle cells were purchased from Kurabo (Osaka, Japan) and maintained in HuMedia-SG2 (Kurabo), supplemented with 5% FCS, 50 ng/ml amphotericin B, 50 μg/ml gentamycin, 0.5 ng/ml human epidermal growth factor, 2 ng/ml human fibroblast growth factor-B and 5 μg/ml insulin. 293T cells were transfected using a standard calcium precipitation protocol. MG132 was purchased from Peptide Institute (Osaka, Japan). NEDD8-activating enzyme inhibitor was purchased from LifeSensors (Malvern, PA, USA).

Immunoprecipitation and western blotting–Immunoprecipitation and western blotting assays were performed as described previously (27). The immunoprecipitates from the indicated cell lysate were resolved by SDS-PAGE and transferred to PVDF membranes (PerkinElmer, Boston, MA, USA). The membranes were then immunoblotted with the different primary antibodies. Immunoreactive proteins were visualized using an enhanced chemiluminescence detection system (Millipore, Bedford, MA). The following primary antibodies were obtained

commercially: anti-JAB1, anti-STAT1, anti-STAT3, anti-CUL1, anti-NRF2 and anti-IFNAR1 antibodies from Santa Cruz Biotechnology (Santa Cruz, CA, USA); anti-phospho-TYK2, anti-phospho-STAT1 and anti-phospho-STAT3 antibodies from Cell Signaling technology (Beverly, MA, USA); anti-CSN2 and anti-CSN4 antibodies from Enzo Life Sciences (Farmingdale, NY, USA); anti-Myc (9E10), anti-FLAG (M2) and anti-actin antibodies from Sigma-Aldrich (St. Louis, MO, USA); anti-TYK2 antibody from BD Biosciences (San Diego, CA, USA); anti-IFNGR1 antibody from abcam (cambridge, MA, USA); anti-IFNAR2 antibody from Thermo scientific/Pierce (Rockford, IL, USA). Horseradish peroxidase-conjugated anti-mouse IgG and anti-rabbit IgG antibodies were purchased from GE Healthcare (Little Chalfont, United Kingdom).

Indirect immunofluorescence microscopy–To analyze subcellular localizations of JAB1 and TYK2 proteins, plasmids encoding FLAG-tagged JAB1 and Myc-tagged TYK2 were transiently transfected into HeLa cells by jetPEI (PolyPlus-transfection, Strasbourg, France). Immunofluorescence staining procedures were performed as described previously(30). The primary antibodies used were rabbit anti-FLAG and mouse anti-Myc antibodies (Sigma-Aldrich, St. Louis, MO, USA). For endogenous protein detection, a rabbit anti-JAB1 antibody (FL-334; Santa Cruz) and a monoclonal anti-TYK2 antibody (clone 51; BD transduction laboratories) were used. The secondary antibodies used were rhodamine-conjugated anti-mouse IgG and FITC-conjugated anti-rabbit IgG (Chemicon, Temecula, CA, USA). DNA was visualized by staining with DAPI (Wako Chemicals, Osaka, Japan). Fluorescent images were acquired using the fluorescent microscope BZ-8000 (Keyence, Osaka, Japan).

Transfection of siRNAs and luciferase assays–The siRNAs used in this study were as follows:

COPS5 (JAB1), 5'-GCUCAGAGUAUCGAUGAAA-3'; TYK2, 5'-GGAGAAACCTCCAATCTCA-3'; COPS2 (CSN2), 5'-GAGGGAAGGTGAATTTGA-3'; COPS4 (CSN4), 5'-GGCAGAGGCTTACATAAAT-3'; NEDD8, 5'-AGGUGGAGCGAAUCAAGGA-3'. HeLa cells were plated on 24-well plates at 2×10^4 cells/well and incubated with an siRNA (10 pmol) - Lipofectamine 2000 (Invitrogen, Carlsbad, CA, USA) mixture at 37 °C for 4 h, followed by the addition of fresh medium containing 10% FCS. HeLa cells were further transfected with or without ISRE-LUC or STAT3-LUC using jetPEI. Twenty-four hours post transfection the cells were harvested and assayed for their luciferase activities using a Dual-Luciferase Reporter Assay System (Promega, Madison, WI, USA).

RNA isolation, reverse-transcription and quantitative real-time PCR–HeLa cells were stimulated with human IFN-α (provided by Dainippon Sumitomo Pharma Co., Ltd., Osaka, Japan) as indicated. After cell harvesting, total RNA samples were extracted using TRI Reagent (Molecular Research Center, Cincinnati, OH, USA). First-strand cDNA was synthesized from 1 μg of total RNA with ReverTra Ace (TOYOBO, Osaka, Japan). Quantitative real-time PCR analysis of mRNA transcripts was carried out using a combination of a KAPA SYBR FAST qPCR master mix (KAPA Biosystems, Woburn, MA, USA) with an Mx3005P real-time PCR system (Stratagene, Santa Clara, CA, USA). Primers used for qPCR were: *IRF1*: 5'-AGCTCAGCTGTGCGAGTGTA-3' (sense), 5'-TAGCTGCTGTGGTCATCAGG-3' (antisense), *PML*: 5'-TTCTGGTGCTTTGAGTGCGAG-3' (sense), 5'-TCACTGTGGCTGCTGTCAAG-3' (antisense), *CXCL11*: 5'-AGAGGACGCTGTCTTTGCAT-3' (sense), 5'-TAAGCCTTGCTTGCTTCGAT-3' (antisense), *IFNAR1*: 5'-TAAGCCTTGCTTGCTTCGAT-3' (sense), 5'-TCTGGAGGACCAATCTGAGC-3'

(antisense), *COPS5 (JAB1)*: 5'-TCTGCTGAAGATGGTGATGC-3' (sense), 5'-GCCAACCTGTTTTGCATTTT-3' (antisense), *ACTB*: 5'-TGTTACCAACTGGGACGACA-3' (sense), 5'-GGGGTGTTGAAGGTCTCAAA-3' (antisense), *APOBEC3G*: 5'-TCCACCCACATTCACTTTCA-3' (sense), 5'-TTCCAAAAGGGAATCACGTC-3' (antisense).

Lentiviral GFP transduction of HeLa cells–The HIV-1-based lentiviral vector pseudotyped with the vesicular stomatitis virus G glycoprotein (VSV-G) (31) was generated as previously described procedures (32) with some modification. In brief, 293T cells were transiently cotransfected with appropriate amounts of the self-inactivating (SIN) lentiviral vector pCSII-CMV-MCS-IRES-hrGFP, the packaging construct (pMDLg/pRRE), the Rev-expressing construct (pRSV-Rev), and the VSV-G–expressing construct (pMD.G). The viral supernatants were collected 72 h after transfection and concentrated 300-fold by ultracentrifugation at 23,200 rpm (P50S2 swing rotor; Hitachi) for 2 h. For infection, HeLa cells were plated on 48-well plates and cultured in DMEM containing 10% FCS and concentrated lentivirus supernatants at a volume of 5 μL per well for 48 h at 37°C in 5% CO2. GFP expression was analyzed using flow cytometry (FACS Calibur, Becton Dickinson).

Cell cycle analysis–Logarithmically growing HeLa cells were incubated with either IFN-α, NAE-inhibitor or both for 24 h. Collected cells were fixed in 90% ethanol and stored overnight at -20 °C. Fixed cells were centrifuged to remove ethanol, and the pellets were resuspended in propidium iodide and RNase A in PBS for 20 min at 37°C. The DNA content of nuclei was analyzed by FACS.

Statistical analysis–Statistical evaluation of differences between populations was determined using Student's *t*-test. Results shown are the means and standard error of the mean (SEM).

RESULTS

Identification of JAB1 as a TYK2-interacting protein–To identify new TYK2-interacting proteins, a yeast two-hybrid screen was performed using the kinase domain of TYK2 fused to the Gal DNA-binding domain (Y2H bait) as bait (Fig. 1A). A human placenta cDNA library was screened. Among a number of positive clones, one clone encoded the N-terminus-truncated portion of previously described JAB1 (Y2H clone) (Fig. 1B). To determine whether this clone encoded a protein able to interact with TYK2 in mammalian cells, the cDNA was subcloned into the mammalian expression vector pCS2-MT. The resulting expression vector produced a protein that interacted with TYK2 in 293T cells (Fig. 1C). Next, we examined the association between TYK2 and JAB1 using the full-length or mutated cDNA. JAB1 MPN domain contains the JAMM-motif that functions as a catalytic site for the CSN isopeptidase activity (23). The JAMM-motif mutant, which harbors a single amino acid substitution from the conserved Asp to Asn at codon 151 (JAB1 D151N), is impaired in its activity. We also generated a JAB1ΔC mutant (JAB1 N), which lacks the nuclear export signal (NES)-containing C-terminal potion of JAB1 (Fig. 1B). Using these JAB1 mutants, we tested whether the JAB1-TYK2 interaction requires an intact JAMM motif. FLAG-tagged wild type or mutant JAB1 with or without TYK2 was introduced into 293T cells and co-immunoprecipitation experiments were performed. As shown in Fig. 1D, the D151N mutant of JAB1 interacted with TYK2 similarly to the wild type JAB1. In addition, JAB1 N interacted rather strongly with TYK2, suggesting that the MPN domain-containing N-terminal portion of JAB1 is sufficient for interacting with TYK2, although the intact JAMM motif is not necessary.

TYK2 domains responsible for the interaction with JAB1 were then determined. We checked whether the kinase domain of TYK2 is required for the interaction with JAB1 using a truncated form of TYK2 that lacks the kinase domain (TYK2ΔKD) (Fig. 1A). The full-length TYK2 or TYK2ΔKD construct was transiently transfected into 293T cells together with the full-length JAB1 construct. Cell lysate was immunoprecipitated with anti-Myc Ab (for TYK2), and immunoblotted with anti-FLAG Ab (for JAB1). Unexpectedly, TYK2ΔKD interacted with JAB1 similarly to the full-length TYK2 (Fig. 1E). Thus, we divided the TYK2 cDNA into four regions (Fig. 1A) and each corresponding TYK2 construct was tested for JAB1-binding ability by immunoprecipitation assay. As shown in Fig. 1F, JAB1 strongly interacted with only TYK2 (600–1086) whereas it interacted very weakly with TYK2 (833–1187), which contains the kinase domain. These data suggest that JAB1 mainly interacts with the region around the pseudokinase domain of TYK2 in mammalian cells.

Binding between endogenous JAB1 and TYK2 as well as involvement of TYK2 activation in this interaction were also investigated. A human cervix carcinoma cell line, HeLa, which expressed both JAB1 and TYK2, was employed, and the cell line was stimulated with IFN-α to activate TYK2. As can be seen in Fig. 1G, JAB1 was present in the TYK2 immunoprecipitates, and their binding was not altered after IFN-α stimulation. Therefore, a part of JAB1 and TYK2 spontaneously associates. in HeLa cells. Finally, subcellular localization of JAB1 and TYK2 was examined. We expressed Myc-tagged TYK2 along with FLAG-tagged JAB1 in HeLa cells, and analysis with immunofluorescence microscopy showed that TYK2 was mostly co-localized with JAB1 throughout the cells (Fig. 1H). Furthermore, endogenous TYK2 co-localized with endogenous JAB1 in cells in the absence or presence of IFN-α stimulation (Fig. 1I). Their co-localization was observed in both nuclei and cytoplasm, as recent studies or a review stated that either TYK2 or

JAB1 localizes in both nuclear and cytoplasmic (20,33,34). Collectively, these data suggest that JAB1 has the ability to interact with TYK2 in mammalian cells.

Knockdown of JAB1 attenuates IFN-α-induced STAT activation–Data for the binding between TYK2 and JAB1 gave rise to a possibility that the interaction might be required for IFN-α-induced signals. We examined whether the selective knockdown of endogenous JAB1 (encoded by *COPS5*) modulates downstream events of IFN-α-stimulation. IFN-α induces the activation of TYK2, which in turn phosphorylates STAT proteins. Although tyrosine phosphorylation of TYK2 was clearly detected in control HeLa cells within 5 min after IFN-α-stimulation, JAB1-knockdown HeLa cells failed to show TYK2 phosphorylation (Fig. 2A). In addition, IFN-α-induced tyrosine phosphorylation of STAT1 and STAT3 was greatly decreased by knockdown of JAB1 (Fig. 2B). When TYK2 expression was reduced by specific TYK2 siRNA, IFN-α-induced phosphorylation of STAT1 almost disappeared (Fig. 2C). Of importance, TYK2-knockdown had larger influence on STAT1 phosphorylation than JAB1-knockdown, and combined knockdown of both JAB1 and TYK2 did not additively reduce STAT1 phosphorylation compared with knockdown of TYK2 alone. Therefore, JAB1 regulates STAT1 activation in a TYK2 expression-dependent manner.

Knockdown of JAB1 attenuates IFN-induced transcriptional activation–The activity of STAT1-containing ISGF3 complex can be measured as luciferase reporter activity using ISRE-Luc, and the activity of STAT3 can be measured as reporter activity using STAT3-Luc (35). We tested effects of JAB1-knockdown on IFN-α-induced activation of STAT1 and STAT3 in HeLa cells. As shown in Fig. 2D, knockdown of JAB1 significantly reduced luciferase activities by ISRE-Luc and STAT3-Luc after IFN-α-stimulation (Fig. 2D). We then examined effects of JAB1 knockdown on IFN-α-induced gene expression. Reverse-transcription quantitative real-time PCR experiments revealed that IFN-α-induced *IRF1, CXCL11* and *PML* mRNA expressions were all significantly reduced in JAB1-knockdown HeLa cells (Fig. 2E). We also analyzed the mRNA levels of *JAB1* itself and *IFNAR1*, which are important components of the IFN-α receptor complex. We found that IFN-α treatment upregulated the *JAB1* mRNA level by approximately 1.8-fold and that JAB1 knockdown did not significantly affect the mRNA level of *IFNAR1*. These results suggest that JAB1 is involved in the optimal IFN-α-induced signaling and gene expression.

JAB1 maintains the protein level of IFNAR1 in HeLa cells–Although JAB1 has been shown to stabilize and destabilize the protein levels of its binding partners (19), we did not observe any changes in the protein levels of TYK2, or downstream STAT proteins by transfection of JAB1 siRNA (Fig. 2A and B). It has been reported that TYK2 constitutively interacts with and stabilizes IFNAR1 (25); therefore, we examined whether knockdown of endogenous JAB1 affects the IFNAR1 protein level. Knockdown of JAB1 induced a significant decrease in the IFNAR1 protein level (Fig. 3A). TYK2 siRNA also induced a decrease in the protein level of IFNAR1; however, the decrease was more severe. We next assessed the cell surface expression level of IFNAR1 by surface biotinylation followed by pull-down using streptavidin-agarose. As shown in Fig. 3B, JAB1 knockdown resulted in the reduction of not only surface but also total IFNAR1 in the cell. Taken together with data that the *IFNAR1* mRNA level was unaffected by JAB1-knockdown (Fig. 2D), JAB1 is likely to regulate IFNAR1 at protein levels.

CUL1 is a component of the SCF-type ubiquitin ligase complex, and its neddylation enhances SCF activity. JAB1 is known to be a component of CSN to remove NEDD8 from Cullin family

6

proteins (deneddylation). As shown in Fig. 3A, knockdown of JAB1 resulted in significant increase of the slower migrating form of CUL1 that is covalently modified by NEDD8. Densitometric analysis revealed that the endogenous IFNAR1 level decreased to 58.5% of control value by knockdown of JAB1 and that CUL1 neddylation was increased from 29.9% in control cells to 44.4% in JAB1-knockdown cells (Fig. 3C). These data suggest that JAB1 may be involved in the IFNAR1 protein level through CSN deneddylation activity.

IFNAR1 protein turnover is mediated by a NEDD8-dependent degradation mechanism–It has been reported that downregulation of either CSN2 or CSN4 subunit is sufficient to impair the CSN function and induce Cullin hyperneddylation (36,37); hence, we downregulated the expression of CSN2 and CSN4 by siRNA to further investigate whether the CSN deneddylation activity affects IFNAR1 protein level. As shown in Fig. 4A, downregulation of either CSN2 or CSN4 induced CUL1 hyperneddylation and resulted in a simultaneous decrease in IFNAR1 protein level compared with the control. Interestingly, targeting the CSN2 or CSN4 subunit by siRNA induced a reduction in JAB1 protein amounts as previously reported results showing that downregulation or deletion of one CSN component can affect the expression of other CSN subunits (37-40).

The increase in CUL1 neddylation generally results in the subsequent activation of SCF ubiquitin E3 ligases and the ubiquitin proteasome system (8-10). Thus, we investigated whether JAB1 knockdown-induced reduction of IFNAR1 protein is recovered by the proteasome inhibitor, MG132. MG132-treatment did not stabilize IFNAR1 protein at all; on the contrary, it induced a larger reduction in IFNAR1 protein, which was accompanied by an apparent increase in the level of neddylated CUL1 protein (Fig. 4B). MG132-induced IFNAR1 degradation and CUL1

hyperneddylation was also observed in cells transfected with control siRNA (Fig. 4B). However, this MG132-induced degradation of IFNAR1 was largely cancelled in cells transfected with NEDD8 siRNA, concomitantly with the efficient reduction in the neddylated form of CUL1 (Fig. 4B). These data indicate that Cullin neddylation, but not the proteasome activity itself, correlates to IFNAR1 degradation.

Ligand stimulation induces the poly-ubiquitination and subsequent degradation of IFNAR1 in an $SCF^{\beta Trcp}$-dependent manner (6). To further examine whether the NEDD8 modification system modulates IFNAR1 stability, the turnover of endogenous IFNAR1 was measured after the treatment with IFN-α for 0–3 h to induce ligand-induced receptor degradation. As shown in Fig. 4C, the time-dependent decrease of IFNAR1 protein after the stimulation with IFN-α was delayed in the NEDD8-knockdown cells. These results suggest that NEDD8 is involved in the proteolysis of IFNAR1.

We also tested effects of JAB1-knockdown on protein levels of other IFN receptors. As shown in Fig. 4D, JAB1 knockdown decreased endogenous IFNGR1 as well as IFNAR1 level, but not IFNAR2 level. Furthermore, JAB1-knockdown also resulted in a decrease of IFN-γ-induced activation of STAT1 in HeLa cells (Fig. 4E). Therefore, JAB1 is involved in the regulation of not only IFN-α- but also IFN-γ-mediated signaling by controlling IFNR protein level

Pharmacological inhibition of the neddylation pathway by NEDD8-activating enzyme inhibitor increases the endogenous IFNAR1 protein level and enhances the susceptibility of HeLa cells to IFN-α–Because the NEDD8-activating enzyme (NAE) inhibitor, MLN4924, effectively inactivates SCF E3 by blocking Cullin neddylation (41), we checked effects of NAE inhibitor on the endogenous IFNAR1 protein level. HeLa cells were treated without or with NAE inhibitor, lysosomal inhibitors (NH_4Cl or

7

Chloroquine) or proteasome inhibitor MG132 for 12 h, and then total cell extracts were prepared for western blot analysis. As shown in Fig. 5A, NAE inhibitor treatment successfully reduced the CUL1 neddylation level, but did not alter the JAB1 amount. In addition, treatment with NAE inhibitor as well as lysosomal inhibitors resulted in the stabilization of endogenous IFNAR1 protein levels, whereas MG132-treatment decreased the IFNAR1 level. These results are consistent with the data showing that the protein turnover of IFNAR1 requires NEDD8 (Fig. 4) and that IFNAR1 is degraded by the lysosomal pathway (42). Next, we investigated whether NAE inhibitor treatment is able to affect the susceptibility of HeLa cells to IFN-α stimulation. HeLa cells were pre-treated without or with NAE inhibitor for 12 h, and then treated with IFN-α. As shown in Fig. 5B, the levels of IFN-α-induced STAT1 phosphorylation were enhanced by the pre-treatment with NAE inhibitor. These results suggest that inhibition of the neddylation pathway can augment STAT1 activation effects of IFN-α by stabilizing the IFNAR1 protein level. We further examined effects of NAE inhibitor on IFN-α-induced antiviral effects in HeLa cells by using a pseudo-type lentiviral infection system (31). As shown in Fig. 5C, a NAE inhibitor clearly enhanced IFN-α-induced anti-viral activity. In addition, gene expression of apolipoprotein B mRNA editing enzyme, catalytic polypeptide-like 3G (APOBEC3G), which is related to the anti-lentiviral activity (43), was highly induced by IFN-α in the presence of a NAE inhibitor (Fig. 5D).

As either IFN-α or NAE inhibitor has been shown to suppress tumor cell viability, we evaluated the combination effect of NAE inhibitor with IFN-α on the growth of HeLa cells. HeLa cells were treated with IFN-α, NAE inhibitor or both. After 48 h, the cell number was determined. As shown in Fig. 5E, in the presence of NAE inhibitor, cultures of HeLa cells with different IFN-α concentrations resulted in a marked and dose-dependent reduction in cell number, while IFN-α treatment alone barely affected. These results suggest that the combination of NAE inhibitor with IFN-α efficiently suppresses HeLa cell viability better than either of these agents alone.

As for the mechanisms of action of NAE inhibitor, it is known to prevent the transition of cells from S-G_2 phase after induction of re-replication stress as well as to induce apoptosis (41,44-46). We also analyzed cell-cycle in HeLa cells treated with IFN-α in the absence or presence of NAE inhibitor. HeLa cells treated with NAE inhibitor newly contained some populations whose DNA contents were over 4N as well as subdiploid (Fig. 5F). When HeLa cells were treated with IFN-α with NAE inhibitor, subdiploid, but not over 4N population significantly increased compared with those treated with NAE inhibitor alone. Therefore, synergical growth suppression by IFN-α and NAE inhibitor seemed to come from the induction of apoptosis.

We also examined effects of NAE inhibitor on endogenous IFNAR1 protein level in non-transformed cell (human smooth muscle) and different cell types (human keratinocyte HaCaT, human hepatoma Hep3B, human T cell leukemia Jurkat and human pre-B cell leukemia NALM-6). As shown in Fig. 5G, treatment of NAE inhibitor increased the IFNAR1 content in these cells as well as HeLa cells. In this situation, expression of TYK2 and JAB1 was not influenced by the treatment with NAE inhibitor while expression of NRF2, a cullin-RING ligase substrate (47) was significantly increased. Therefore, this NEDDylaton effect on IFNAR1 is likely to be general.

DISCUSSION

In this study, we identified JAB1 as a new TYK2 binding partner. Because TYK2 has

important roles in the stabilization of the IFN receptor complex and in the IFN-α-induced signal transduction, we investigated whether JAB1 is also involved in these processes. COPS5 (JAB1) siRNA-treated cells exhibited reduced responses to IFN-α as revealed by the analysis of the phosphorylation of TYK2, STAT1 and STAT3, and of the IFN-α-induced gene expression. These data indicate that JAB1 has a positive role in the IFN-α-induced cell responses.

Downregulation and degradation of IFNAR1 is one of the pivotal mechanisms to limit the extent and duration of cellular responses to IFN-α. The involvement of the E3 ligase complex SCF$^{β-Trcp}$-mediated ubiquitination of IFNAR1 in the turnover of IFNAR1 has been described previously (6). The ubiquitination of IFNAR1 promotes its interaction with clathrin and stimulates receptor internalization and subsequent lysosomal degradation (48). The ubiquitin ligase activity of the SCF complex is controlled by neddylation and deneddylation of Cullin subunits (12). Collectively, these previous observations have implicated the involvement of the neddylation/deneddylation mechanism in the regulation of IFNAR1 protein stability. Because JAB1 is also known as CSN5, which acts in the removal of NEDD8 from Cullins by serving as a catalyzing center of CSN (23), we tested the effect of JAB1 knockdown on the protein level of IFNAR1 and demonstrated that JAB1 is involved in the regulation of IFNAR1 protein stability. Importantly, the decrease in IFNAR1 protein levels induced by JAB1-knockdown were accompanied by activation of the SCF complex containing CUL1, as judged by a notable enhancement in CUL1 neddylation level. In addition, knockdown of either CSN2 or CSN4, which are also CSN subunits, resulted in a simultaneous induction of IFNAR1 decrease and CUL1 hyperneddylation in the cell. Moreover, knockdown of NEDD8 or inhibition of neddylation by NAE inhibitor resulted in an increase in IFNAR1 protein with concomitant reduction in neddylated CUL1. These results indicate that the neddylation pathway is involved in the proteolysis of IFNAR1, and that the CSN deneddylating activity contributes to the stability of IFNAR1 protein.

Interestingly, treatment with the proteasomal inhibitor, MG132, induced a notable decrease in endogenous IFNAR1 protein (Fig. 4B). This result was highly reproducible. The most possible explanation for this phenomenon would be the unfolded protein response (UPR) by undegraded polypeptides in the endoplasmic reticulum (ER), because previous studies have shown that proteasomal inhibitors including MG132 are known to trigger ER-stress (49,50) and that ER-stress/UPR is correlated well with degradation of IFNAR1 in cells (51-53). In addition, UPR stimuli-induced degradation of IFNAR1 is known to be mediated by recruitment of SCF$^{β-Trcp}$, ubiquitination, endocytosis and degradation (51). Thus, our results that MG132-induced degradation of IFNAR1 was enhanced by JAB1 knockdown and suppressed by NEDD8 knockdown (Fig. 4B) well suit the explanation stated above and seem to indicate the importance of neddylation/deneddylation control in the ligand-independent IFNAR1 degradation.

Along with the effects on ER-stress, MG132 might have additional effects on SCF activation in cells, as MG132-treatment induced a remarkable increase in the level of neddylated CUL1 protein (Fig. 4B). It has been reported that the neddylation-defective CUL1 K720R mutant protein is more stable than wild type in cells (54), indicating that CUL1 is degraded through the ubiquitin-proteasome pathway preferentially in the neddylated form; thus, the inhibition of CUL1 degradation by MG132 seems to induce preferential accumulation of neddylated CUL1, leading to enhanced activation of SCF ligase activity as well as IFNAR1 degradation.

TYK2 has been reported to constitutively

9

associate with IFNAR1 and stabilize its cell surface expression by masking the conserved linear endocytic motif in the cytoplasmic tail of IFNAR1 through the protein-protein interaction (25). In accordance with this report, we showed that the basal IFNAR1 protein level was very low after transfection of TYK2 siRNA, indicating that TYK2 is the primarily important factor for stabilizing the basal level of IFNAR1. We demonstrated that JAB1 interacted with TYK2 constitutively and that JAB1 knockdown induced about 40% decrease of the amount of IFNAR1 protein. These data revealed the role of JAB1 in fine-tuning the basal IFNAR1 level in the presence of TYK2. Indeed, in the absence of TYK2 protein, we did not observe any changes in IFN-α-induced STAT1 phosphorylation after .

knockdown of JAB1 (Fig. 2C).

The NAE inhibitor, MLN4924, effectively inactivates SCF E3 by blocking Cullin neddylation (41), and thereby suppresses cell cycle progression. NAE inhibitor has shown potent activity in *in vitro* and *in vivo* solid tumor models. In this study, we showed that combination of NAE inhibitor with IFN-α efficiently suppresses HeLa cell viability better than either of these agents alone, thus the combination of IFN-α and NAE inhibitor may be a good strategy against cancer that is resistant to IFN-α or NAE treatment alone.

In summary, our finding that JAB1 has a role in stabilizing IFNAR1 protein through antagonizing NEDD8 modification provides new insight into the regulation mechanism of type I IFN signaling.

REFERENCES

1. Stark, G. R., and Darnell, J. E., Jr. (2012) The JAK-STAT pathway at twenty *Immunity* **36**, 503-514
2. Pestka, S., Krause, C. D., and Walter, M. R. (2004) Interferons, interferon-like cytokines, and their receptors *Immunol. Rev.* **202**, 8-32
3. Hwang, S. Y., Hertzog, P. J., Holland, K. A., Sumarsono, S. H., Tymms, M. J., Hamilton, J. A., Whitty, G., Bertoncello, I., and Kola, I. (1995) A null mutation in the gene encoding a type I interferon receptor component eliminates antiproliferative and antiviral responses to interferons alpha and beta and alters macrophage responses *Proc. Natl. Acad. Sci. USA.* **92**, 11284-11288
4. Constantinescu, S. N., Croze, E., Wang, C., Murti, A., Basu, L., Mullersman, J. E., and Pfeffer, L. M. (1994) Role of interferon alpha/beta receptor chain 1 in the structure and transmembrane signaling of the interferon alpha/beta receptor complex *Proc. Natl. Acad. Sci. USA.* **91**, 9602-9606
5. Muller, U., Steinhoff, U., Reis, L. F., Hemmi, S., Pavlovic, J., Zinkernagel, R. M., and Aguet, M. (1994) Functional role of type I and type II interferons in antiviral defense *Science* **264**, 1918-1921
6. Kumar, K. G., Tang, W., Ravindranath, A. K., Clark, W. A., Croze, E., and Fuchs, S. Y. (2003) SCF(HOS) ubiquitin ligase mediates the ligand-induced down-regulation of the interferon-alpha receptor *EMBO J.* **22**, 5480-5490
7. Liu, J., Plotnikov, A., Banerjee, A., Suresh Kumar, K. G., Ragimbeau, J., Marijanovic, Z., Baker, D. P., Pellegrini, S., and Fuchs, S. Y. (2008) Ligand-independent pathway that controls stability of interferon alpha receptor *Biochem. Biophys. Res. Commun.* **367**, 388-393
8. Cardozo, T., and Pagano, M. (2004) The SCF ubiquitin ligase: insights into a molecular machine *Nat. Rev. Mol. Cell. Biol.* **5**, 739-751
9. Petroski, M. D., and Deshaies, R. J. (2005) Function and regulation of cullin-RING ubiquitin ligases *Nat. Rev. Mol. Cell. Biol.* **6**, 9-20
10. Willems, A. R., Schwab, M., and Tyers, M. (2004) A hitchhiker's guide to the cullin ubiquitin ligases: SCF and its kin *Biochim. Biophys. Acta* **1695**, 133-170
11. Saha, A., and Deshaies, R. J. (2008) Multimodal activation of the ubiquitin ligase SCF by Nedd8 conjugation *Mol. Cell* **32**, 21-31
12. Soucy, T. A., Smith, P. G., and Rolfe, M. (2009) Targeting NEDD8-activated cullin-RING ligases for the treatment of cancer *Clin. Cancer Res.* **15**, 3912-3916
13. Furukawa, M., Zhang, Y., McCarville, J., Ohta, T., and Xiong, Y. (2000) The CUL1 C-terminal sequence and ROC1 are required for efficient nuclear accumulation, NEDD8 modification, and ubiquitin ligase activity of CUL1 *Mol. Cell. Biol.* **20**, 8185-8197
14. Read, M. A., Brownell, J. E., Gladysheva, T. B., Hottelet, M., Parent, L. A., Coggins, M. B., Pierce, J. W., Podust, V. N., Luo, R. S., Chau, V., and Palombella, V. J. (2000) Nedd8 modification of cul-1 activates SCF(beta(TrCP))-dependent ubiquitination of IkappaBalpha *Mol. Cell. Biol.* **20**, 2326-2333
15. Wu, K., Chen, A., and Pan, Z. Q. (2000) Conjugation of Nedd8 to CUL1 enhances the ability of the ROC1-CUL1 complex to promote ubiquitin polymerization *J. Biol. Chem.* **275**, 32317-32324
16. Cope, G. A., and Deshaies, R. J. (2003) COP9 signalosome: a multifunctional regulator of SCF

and other cullin-based ubiquitin ligases *Cell* **114**, 663-671

17.   Wolf, D. A., Zhou, C., and Wee, S. (2003) The COP9 signalosome: an assembly and maintenance platform for cullin ubiquitin ligases? *Nat. Cell Biol.* **5**, 1029-1033

18.   Schwechheimer, C. (2004) The COP9 signalosome (CSN): an evolutionary conserved proteolysis regulator in eukaryotic development *Biochim. Biophys. Acta* **1695**, 45-54

19.   Wei, N., Serino, G., and Deng, X. W. (2008) The COP9 signalosome: more than a protease *Trends Biochem. Sci.* **33**, 592-600

20.   Wei, N., and Deng, X. W. (2003) The COP9 signalosome *Annu. Rev. Cell Dev. Biol.* **19**, 261-286

21.   Lyapina, S., Cope, G., Shevchenko, A., Serino, G., Tsuge, T., Zhou, C., Wolf, D. A., Wei, N., and Deshaies, R. J. (2001) Promotion of NEDD-CUL1 conjugate cleavage by COP9 signalosome *Science* **292**, 1382-1385

22.   Schwechheimer, C., Serino, G., Callis, J., Crosby, W. L., Lyapina, S., Deshaies, R. J., Gray, W. M., Estelle, M., and Deng, X. W. (2001) Interactions of the COP9 signalosome with the E3 ubiquitin ligase SCFTIRI in mediating auxin response *Science* **292**, 1379-1382

23.   Cope, G. A., Suh, G. S., Aravind, L., Schwarz, S. E., Zipursky, S. L., Koonin, E. V., and Deshaies, R. J. (2002) Role of predicted metalloprotease motif of Jab1/Csn5 in cleavage of Nedd8 from Cul1 *Science* **298**, 608-611

24.   Gauzzi, M. C., Barbieri, G., Richter, M. F., Uze, G., Ling, L., Fellous, M., and Pellegrini, S. (1997) The amino-terminal region of Tyk2 sustains the level of interferon alpha receptor 1, a component of the interferon alpha/beta receptor *Proc. Natl. Acad. Sci. USA.* **94**, 11839-11844

25.   Kumar, K. G., Varghese, B., Banerjee, A., Baker, D. P., Constantinescu, S. N., Pellegrini, S., and Fuchs, S. Y. (2008) Basal ubiquitin-independent internalization of interferon alpha receptor is prevented by Tyk2-mediated masking of a linear endocytic motif *J. Biol. Chem.* **283**, 18566-18572

26.   Minegishi, Y., Saito, M., Morio, T., Watanabe, K., Agematsu, K., Tsuchiya, S., Takada, H., Hara, T., Kawamura, N., Ariga, T., Kaneko, H., Kondo, N., Tsuge, I., Yachie, A., Sakiyama, Y., Iwata, T., Bessho, F., Ohishi, T., Joh, K., Imai, K., Kogawa, K., Shinohara, M., Fujieda, M., Wakiguchi, H., Pasic, S., Abinun, M., Ochs, H. D., Renner, E. D., Jansson, A., Belohradsky, B. H., Metin, A., Shimizu, N., Mizutani, S., Miyawaki, T., Nonoyama, S., and Karasuyama, H. (2006) Human tyrosine kinase 2 deficiency reveals its requisite roles in multiple cytokine signals involved in innate and acquired immunity *Immunity* **25**, 745-755

27.   Muromoto, R., Sugiyama, K., Takachi, A., Imoto, S., Sato, N., Yamamoto, T., Oritani, K., Shimoda, K., and Matsuda, T. (2004) Physical and functional interactions between Daxx and DNA methyltransferase 1-associated protein, DMAP1 *J. Immunol.* **172**, 2985-2993

28.   Haro, T., Shimoda, K., Kakumitsu, H., Kamezaki, K., Numata, A., Ishikawa, F., Sekine, Y., Muromoto, R., Matsuda, T., and Harada, M. (2004) Tyrosine kinase 2 interacts with and phosphorylates receptor for activated C kinase-1, a WD motif-containing protein *J. Immunol.* **173**, 1151-1157

29.   Yamakami, M., Yoshimori, T., and Yokosawa, H. (2003) Tom1, a VHS domain-containing protein, interacts with tollip, ubiquitin, and clathrin *J. Biol. Chem.* **278**, 52865-52872

30.   Muromoto, R., Ishida, M., Sugiyama, K., Sekine, Y., Oritani, K., Shimoda, K., and Matsuda, T. (2006) Sumoylation of Daxx regulates IFN-induced growth suppression of B lymphocytes and the hormone receptor-mediated transactivation *J. Immunol.* **177**, 1160-1170

31. Miyoshi, H., Blomer, U., Takahashi, M., Gage, F. H., and Verma, I. M. (1998) Development of a self-inactivating lentivirus vector *J Virol* **72**, 8150-8157

32. Shibuya, K., Shirakawa, J., Kameyama, T., Honda, S., Tahara-Hanaoka, S., Miyamoto, A., Onodera, M., Sumida, T., Nakauchi, H., Miyoshi, H., and Shibuya, A. (2003) CD226 (DNAM-1) is involved in lymphocyte function-associated antigen 1 costimulatory signal for naive T cell differentiation and proliferation *J Exp Med* **198**, 1829-1839

33. Ragimbeau, J., Dondi, E., Vasserot, A., Romero, P., Uze, G., and Pellegrini, S. (2001) The receptor interaction region of Tyk2 contains a motif required for its nuclear localization *J. Biol. Chem.* **276**, 30812-30818

34. Ahmed, C. M., Noon-Song, E. N., Kemppainen, K., Pascalli, M. P., and Johnson, H. M. (2013) Type I IFN receptor controls activated TYK2 in the nucleus: implications for EAE therapy *J Neuroimmunol* **254**, 101-109

35. Muromoto, R., Okabe, K., Fujimuro, M., Sugiyama, K., Yokosawa, H., Seya, T., and Matsuda, T. (2006) Physical and functional interactions between STAT3 and Kaposi's sarcoma-associated herpesvirus-encoded LANA *FEBS Lett.* **580**, 93-98

36. Pearce, C., Hayden, R. E., Bunce, C. M., and Khanim, F. L. (2009) Analysis of the role of COP9 Signalosome (CSN) subunits in K562; the first link between CSN and autophagy *BMC Cell Biol.* **10**, 31

37. Denti, S., Fernandez-Sanchez, M. E., Rogge, L., and Bianchi, E. (2006) The COP9 signalosome regulates Skp2 levels and proliferation of human cells *J. Biol. Chem.* **281**, 32188-32196

38. Welteke, V., Eitelhuber, A., Duwel, M., Schweitzer, K., Naumann, M., and Krappmann, D. (2009) COP9 signalosome controls the Carma1-Bcl10-Malt1 complex upon T-cell stimulation *EMBO Rep.* **10**, 642-648

39. Schweitzer, K., Bozko, P. M., Dubiel, W., and Naumann, M. (2007) CSN controls NF-kappaB by deubiquitinylation of IkappaBalpha *EMBO J.* **26**, 1532-1541

40. Menon, S., Chi, H., Zhang, H., Deng, X. W., Flavell, R. A., and Wei, N. (2007) COP9 signalosome subunit 8 is essential for peripheral T cell homeostasis and antigen receptor-induced entry into the cell cycle from quiescence *Nat. Immunol.* **8**, 1236-1245

41. Soucy, T. A., Smith, P. G., Milhollen, M. A., Berger, A. J., Gavin, J. M., Adhikari, S., Brownell, J. E., Burke, K. E., Cardin, D. P., Critchley, S., Cullis, C. A., Doucette, A., Garnsey, J. J., Gaulin, J. L., Gershman, R. E., Lublinsky, A. R., McDonald, A., Mizutani, H., Narayanan, U., Olhava, E. J., Peluso, S., Rezaei, M., Sintchak, M. D., Talreja, T., Thomas, M. P., Traore, T., Vyskocil, S., Weatherhead, G. S., Yu, J., Zhang, J., Dick, L. R., Claiborne, C. F., Rolfe, M., Bolen, J. B., and Langston, S. P. (2009) An inhibitor of NEDD8-activating enzyme as a new approach to treat cancer *Nature* **458**, 732-736

42. Ragimbeau, J., Dondi, E., Alcover, A., Eid, P., Uze, G., and Pellegrini, S. (2003) The tyrosine kinase Tyk2 controls IFNAR1 cell surface expression *EMBO J.* **22**, 537-547

43. Chiu, Y. L., and Greene, W. C. (2008) The APOBEC3 cytidine deaminases: an innate defensive network opposing exogenous retroviruses and endogenous retroelements *Annu Rev Immunol* **26**, 317-353

44. Milhollen, M. A., Narayanan, U., Soucy, T. A., Veiby, P. O., Smith, P. G., and Amidon, B. (2011) Inhibition of NEDD8-activating enzyme induces rereplication and apoptosis in human tumor cells consistent with deregulating CDT1 turnover *Cancer Res* **71**, 3042-3051

45. Lin, J. J., Milhollen, M. A., Smith, P. G., Narayanan, U., and Dutta, A. (2010) NEDD8-targeting drug MLN4924 elicits DNA rereplication by stabilizing Cdt1 in S phase, triggering checkpoint activation, apoptosis, and senescence in cancer cells *Cancer Res* **70**, 10310-10320

46. Blank, J. L., Liu, X. J., Cosmopoulos, K., Bouck, D. C., Garcia, K., Bernard, H., Tayber, O., Hather, G., Liu, R., Narayanan, U., Milhollen, M. A., and Lightcap, E. S. (2013) Novel DNA damage checkpoints mediating cell death induced by the NEDD8-activating enzyme inhibitor MLN4924 *Cancer Res* **73**, 225-234

47. Kobayashi, A., Kang, M. I., Okawa, H., Ohtsuji, M., Zenke, Y., Chiba, T., Igarashi, K., and Yamamoto, M. (2004) Oxidative stress sensor Keap1 functions as an adaptor for Cul3-based E3 ligase to regulate proteasomal degradation of Nrf2 *Mol Cell Biol* **24**, 7130-7139

48. Kumar, K. G., Barriere, H., Carbone, C. J., Liu, J., Swaminathan, G., Xu, P., Li, Y., Baker, D. P., Peng, J., Lukacs, G. L., and Fuchs, S. Y. (2007) Site-specific ubiquitination exposes a linear motif to promote interferon-alpha receptor endocytosis *J. Cell. Biol.* **179**, 935-950

49. Bush, K. T., Goldberg, A. L., and Nigam, S. K. (1997) Proteasome inhibition leads to a heat-shock response, induction of endoplasmic reticulum chaperones, and thermotolerance *J Biol Chem* **272**, 9086-9092

50. Lee, A. H., Iwakoshi, N. N., Anderson, K. C., and Glimcher, L. H. (2003) Proteasome inhibitors disrupt the unfolded protein response in myeloma cells *Proc Natl Acad Sci U S A* **100**, 9946-9951

51. Bhattacharya, S., HuangFu, W. C., Liu, J., Veeranki, S., Baker, D. P., Koumenis, C., Diehl, J. A., and Fuchs, S. Y. (2010) Inducible priming phosphorylation promotes ligand-independent degradation of the IFNAR1 chain of type I interferon receptor *J Biol Chem* **285**, 2318-2325

52. Minakshi, R., Padhan, K., Rani, M., Khan, N., Ahmad, F., and Jameel, S. (2009) The SARS Coronavirus 3a protein causes endoplasmic reticulum stress and induces ligand-independent downregulation of the type 1 interferon receptor *PLoS One* **4**, e8342

53. Liu, J., HuangFu, W. C., Kumar, K. G., Qian, J., Casey, J. P., Hamanaka, R. B., Grigoriadou, C., Aldabe, R., Diehl, J. A., and Fuchs, S. Y. (2009) Virus-induced unfolded protein response attenuates antiviral defenses via phosphorylation-dependent degradation of the type I interferon receptor *Cell Host Microbe* **5**, 72-83

54. Morimoto, M., Nishida, T., Nagayama, Y., and Yasuda, H. (2003) Nedd8-modification of Cul1 is promoted by Roc1 as a Nedd8-E3 ligase and regulates its stability *Biochem. Biophys. Res. Commun.* **301**, 392-398

FIGURE LEGENDS

FIGURE 1. JAB1 with TYK2 interactions. (A) Schematic representation of TYK2 constructs. (B) Schematic representation of JAB1 constructs. (C) Myc-tagged Y2H clone was transfected into 293T cells with the untagged TYK2 construct. Cell extracts were subjected to immunoprecipitation with anti-Myc antibody followed by immunoblotting with anti-TYK2 antibody. (D) FLAG-JAB1 wild type (WT), C-terminal deletion mutant (N) or JAMM mutant (D151N) was transfected into 293T cells together with the Myc-tagged TYK2 construct as indicated. Cell extracts were subjected to immunoprecipitation with anti-FLAG tag antibody followed by immunoblotting with anti-Myc-tag antibody. (E and F) Mapping of the JAB1-interacting region on TYK2. FLAG-JAB1 was transfected into 293T cells with the TYK2 constructs. Cell extracts were subjected to immunoprecipitation with anti-Myc antibody followed by immunoblotting with anti-FLAG antibody. (G) Interaction between endogenous JAB1 and TYK2 in HeLa cells. HeLa cells (2×10^8 cells) were stimulated with or without IFN-α (1000 U/ml) for 5 min. The cells were then lysed, immunoprecipitated with control IgG or anti-TYK2 antibody, and subjected to western blot analysis for JAB1 and TYK2. An aliquot of total cell lysate was also analyzed. (H) Co-localization of JAB1 and TYK2 in HeLa cells. FLAG-JAB1 and Myc-TYK2 were co-transfected into HeLa cells. After cells had been fixed, localization of FLAG-JAB1 and Myc-TYK2 was analyzed by immunocytochemistry with anti-FLAG and anti-Myc antibodies as described in Materials and methods. DAPI was used for nuclear staining. (I) Co-localization of endogenous JAB1 and endogenous TYK2 in HeLa cells. HeLa cells were left untreated or treated with IFN-α (1000 U/ml) for 30 min. The cells were fixed and stained with anti-TYK2 and anti-JAB1 antibodies. For negative control staining, cells were incubated without primary antibody.

FIGURE 2. Knockdown of JAB1 attenuates TYK2 and STAT activation induced by IFN-α. (A and B) HeLa cells were transfected with control or JAB1 (encoded by *COPS5*) siRNA, and the cells were stimulated with IFN-α (1000 U/ml) for the indicated periods. The cells were lysed, and lysate was immunoblotted with the indicated antibodies. (C) HeLa cells were transfected with JAB1 siRNA, TYK2 siRNA or together as indicated, and cells were stimulated with IFN-α (1000 U/ml) for 30 min. The cells were lysed, and lysate was immunoblotted with the indicated antibodies. (D) Knockdown of JAB1 attenuates transcriptional activation induced by IFN-α. HeLa cells were transfected with control or COPS5 siRNA. The cells were then transfected with ISRE-LUC or STAT3-LUC using jetPEI. The cells were stimulated with IFN-α (1000 U/ml) 24 h after transfection. Twelve hours after stimulation, the cells were harvested and the luciferase activities were measured. Results are the mean of three independent experiments. The error bars represent the SEM (n=3). *$P < 0.05$. (E) HeLa cells were treated with control or COPS5 siRNA. Cells were then stimulated with IFN-α (1000 U/ml) for 2 h. Total RNA samples isolated from these cells were subjected to quantitative real-time PCR analysis using *IRF1*, *CXCL11*, *PML*, *IFNAR1*, *COPS5* or *ACTB* primers. Data represent the levels of mRNA normalized to the *ACTB* internal control and are expressed relative to the value of control siRNA-treated samples without IFN-α stimulation. Results are the mean of three independent experiments. The error bars represent the SEM (n=3). *$P < 0.05$ **$P < 0.01$

FIGURE 3. JAB1 maintains the protein level of IFNAR1. (A) HeLa cells were transfected with control, JAB1 or TYK2 siRNA. The cells were lysed, and lysate was immunoblotted with the indicated antibodies.

(B) Biotinylated HeLa cell surface proteins were precipitated with streptavidin-agarose beads and analyzed by immunoblotting with IFNAR1 antibody. Total cell lysates were immunoblotted with the indicated antibodies. (C) Densitometric analysis of western blots shown in A. IFNAR1 protein band intensity was quantified and normalized to the density of the β-actin band and data are expressed as a percentage relative to control, which was set at 100% (left panel). The intensity of neddylated and unmodified CUL1 bands was quantified by densitometry, and the percentage of neddylated to the total of neddylated and unmodified CUL1 band is indicated (right panel). Results are the mean of eight independent experiments. The error bars represent the SEM (n=8). ***$P < 0.005$.

FIGURE 4. NEDD8 is involved in the IFNAR1 turnover. (A) Effect of the knockdown of CSN components on the level of IFNAR1 protein. HeLa cells were transfected with control, JAB1, CSN2 or CSN4 siRNA. Forty-eight hours after transfection, the cells were lysed and lysate was immunoblotted with the indicated antibodies. (B) Effect of MG132 treatment on the level of IFNAR1 protein. HeLa cells were transfected with control, JAB1 or NEDD8 siRNA. Forty-eight hours after transfection, proteasome inhibitor MG132 (10 μM) was added and incubated for 5 h. The cells were then lysed and subjected to western blot analysis. (C) Ligand-induced degradation of IFNAR1 is slowed down by knockdown of NEDD8. HeLa cells were transfected with control or NEDD8 siRNA. Forty-eight hours after transfection, IFN-α (1000 U/ml) was added and incubated for the indicated periods. The cells were then lysed and subjected to western blot analysis. (D) HeLa cells were transfected with control or JAB1 siRNA. The cells were lysed, and lysate was immunoblotted with the indicated IFNR antibodies. (E) HeLa cells were transfected with control or JAB1 siRNA, and the cells were stimulated with IFN-γ (10 ng/ml) for the indicated periods. The cells were lysed, and lysate was immunoblotted with the indicated antibodies.

FIGURE 5. NAE inhibitor treatment increases endogenous IFNAR1 protein level and renders HeLa cells susceptible to growth suppressive effects by IFN-α. (A) Effect of the inhibitors on the level of IFNAR1 protein. HeLa cells were treated with NAE inhibitor (1 μM), NH4Cl (20 mM), Chloroquine (50 μM), or MG132 (10 μM) for 12 h. The cells were lysed, and lysate was immunoblotted with the indicated antibodies. (B) Effect of the NAE inhibitor pretreatment on IFN-α effects. HeLa cells were treated with DMSO control or NAE inhibitor (1 μM) for 12 h and then stimulated with IFN-α (1000 U/ml) for the indicated periods. The cells were lysed, and lysate was immunoblotted. Right graph shows the densitometric analysis of western blots. Phospho-STAT1 protein band intensity was quantified and normalized to the density of the total-STAT1 band and data are expressed as a percentage relative to DMSO-treated cells stimulated with IFN-α (15 min), which was set at 100%. Results are the mean of five independent experiments. The error bars represent the SEM (n=5). *$P < 0.05$. (C) HIV-1-based lentiviral particles expressing GFP (Lenti-GFP) were prepared and assayed for transduction of GFP into HeLa cells. For infection, HeLa cells were pretreated with either IFN-α (1000 U/ml), NAE inhibitor (1 μM) or IFN-α plus NAE inhibitor for 3 h and then cultured in medium containing lentivirus particles for 48 h. GFP expression was analyzed by flow cytometry. Representative flow cytometric dot plots are shown (left panels). Right graph shows the total % of GFP-positive cells. Results are the mean of three independent experiments. The error bars represent the SEM (n=3). *$P < 0.05$. (D) HeLa cells treated as in C were collected and total RNA samples isolated from these cells were subjected to quantitative real-time PCR analysis using *APOBEC3G* or *ACTB* primers. Data represent the levels normalized to the *ACTB* internal control and are expressed relative to the value of control samples. Results are the mean of three

independent experiments. The error bars represent the SEM (n=3). *P < 0.05 **P < 0.01. (E) HeLa cells (5×10^3) were treated with the indicated concentrations of IFN-α, NAE inhibitor or both for 48 h, and the cell viability was determined by Cell Counting Kit-8. Results are the mean of three independent experiments. The error bars represent the SEM (n=3) *P < 0.05 **P < 0.01 ***P < 0.005. (F) HeLa cells were treated with IFN-α (1000 U/ml) in the absence or presence of NAE inhibitor (1 μM) for 24 h. DNA profiles were analysed by flow cytometry. The percentage of re-replicated cells (the DNA content higher than 4N) and of dead (sub-G1) are shown. Results are the mean of three independent experiments. The error bars represent the SEM (n=3). *P < 0.05 ***P < 0.005. (G) The effect of NAE inhibitor on the level of IFNAR1 protein in various types of cells. Non-transformed cell (human smooth muscle) and different cell types (human keratinocyte HaCaT, human hepatoma Hep3B, human T cell leukemia Jurkat and human pre-B cell leukemia NALM-6) as well as HeLa cells were treated with NAE inhibitor (1 μM) for 12 h. The cells were lysed, and lysate was immunoblotted with the indicated antibodies.
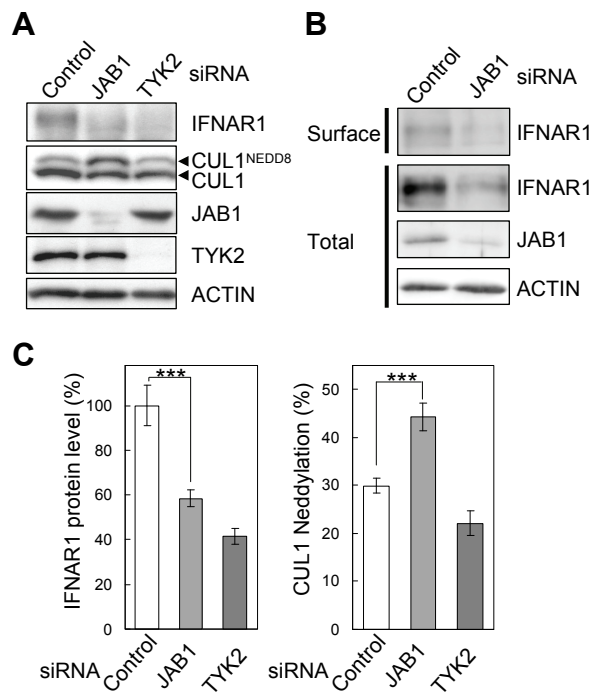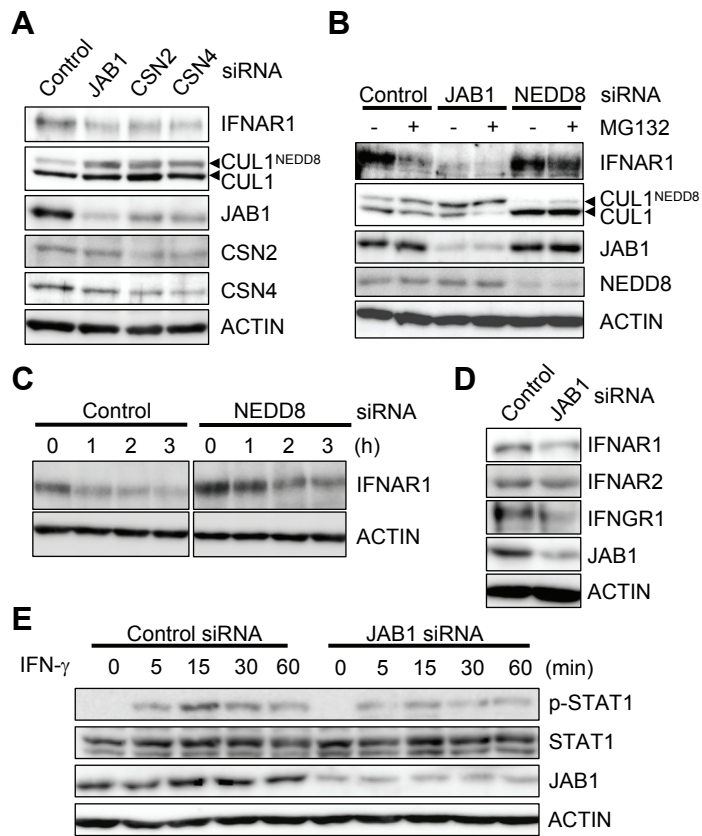
FIGURE 1
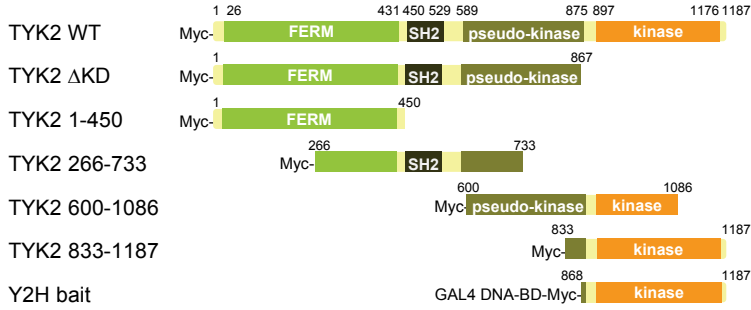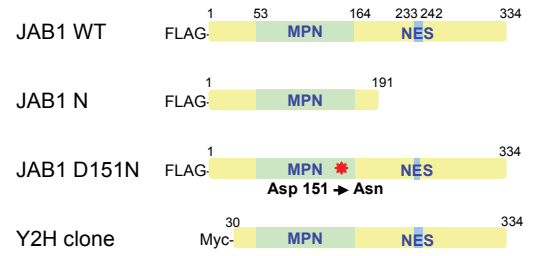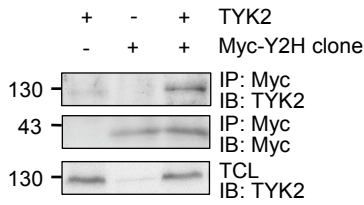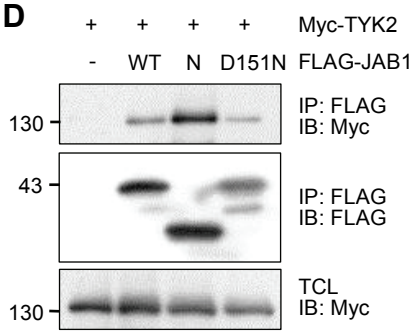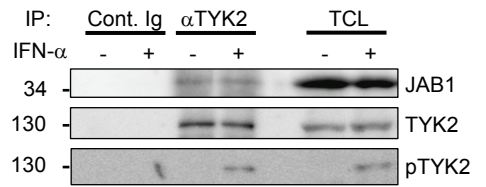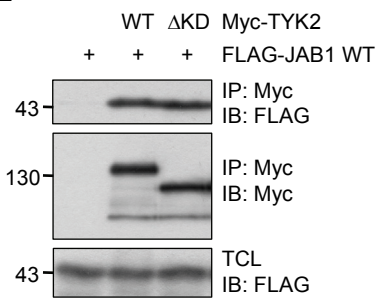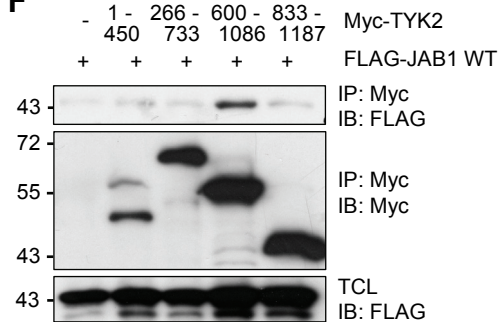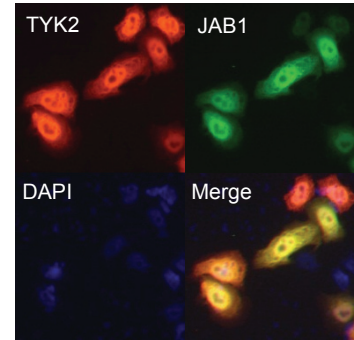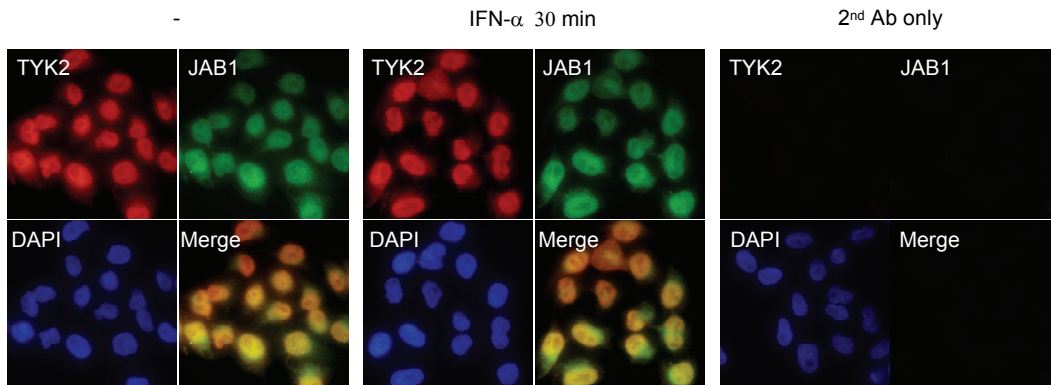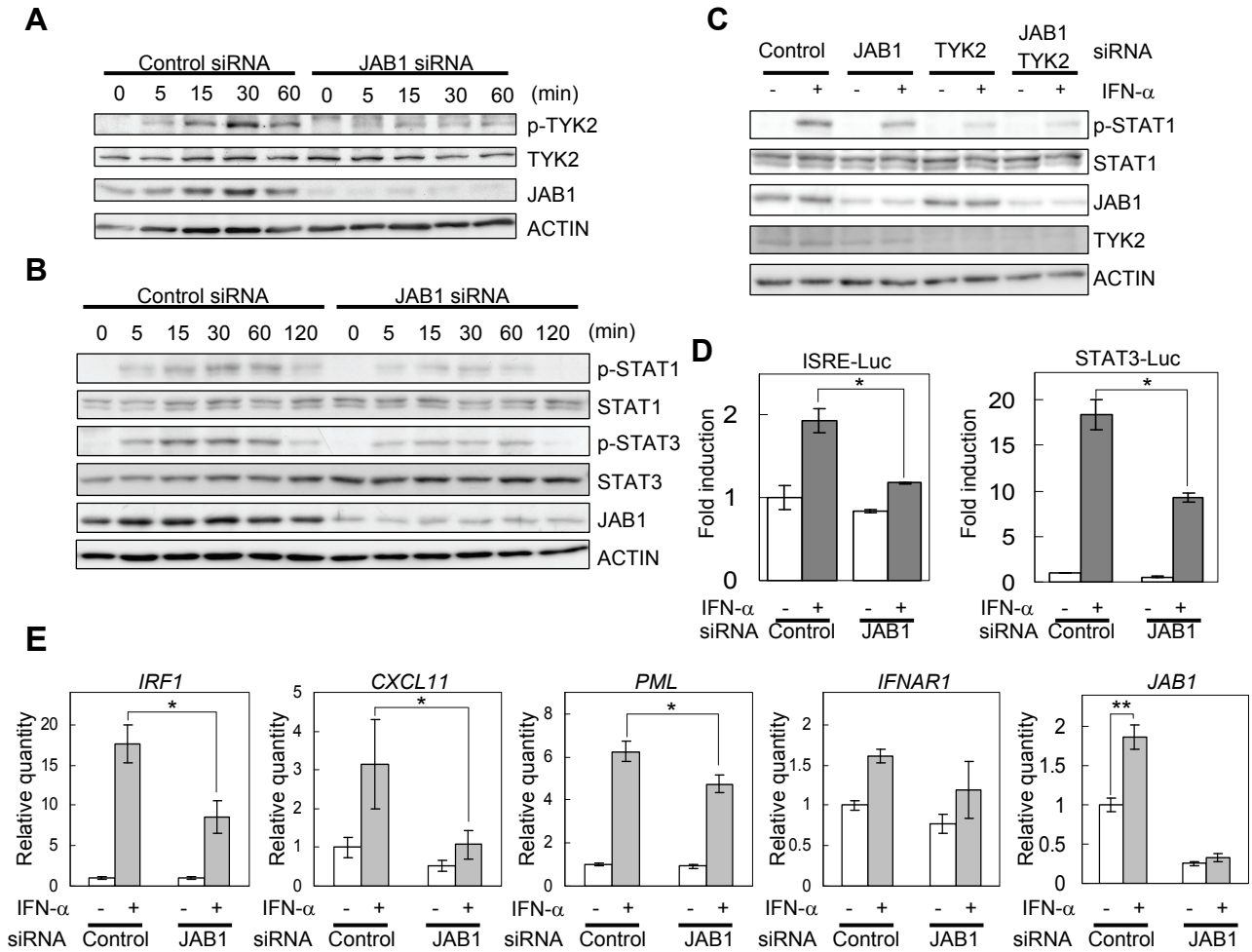
FIGURE 2

FIGURE 3

FIGURE 4

FIGURE 5